Technical evaluation of Siemens Inspiration PRIME with VB30L software

NHS Breast Screening Programme Equipment Report 1503

March 2016

Public Health England leads the NHS Screening Programmes

About Public Health England

Public Health England exists to protect and improve the nation's health and wellbeing, and reduce health inequalities. It does this through world-class science, knowledge and intelligence, advocacy, partnerships and the delivery of specialist public health services. PHE is an operationally autonomous executive agency of the Department of Health.

Public Health England, Wellington House, 133-155 Waterloo Road, London SE1 8UG
Tel: 020 7654 8000   www.gov.uk/phe
Twitter: @PHE_uk   Facebook: www.facebook.com/PublicHealthEngland

About PHE Screening

Screening identifies apparently healthy people who may be at increased risk of a disease or condition, enabling earlier treatment or better informed decisions. National population screening programmes are implemented in the NHS on the advice of the UK National Screening Committee (UK NSC), which makes independent, evidence-based recommendations to ministers in the four UK countries. The Screening Quality Assurance Service ensures programmes are safe and effective by checking that national standards are met. PHE leads the NHS Screening Programmes and hosts the UK NSC secretariat.

PHE Screening, Floor 2, Zone B, Skipton House, 80 London Road, London SE1 6LH
www.gov.uk/topic/population-screening-programmes
Twitter: @PHE_Screening   Blog: phescreening.blog.gov.uk

Prepared by: JM Oduko, CJ Strudley, KC Young
For queries relating to this document, please contact: PHE.screeninghelpdesk@nhs.net

Corporate member of
Plain English Campaign
Committed to clearer
communication
339

Acknowledgements

Document Information	
Title	Technical evaluation of Siemens Inspiration PRIME with VB30L software
Policy/document type	Equipment Report 1503
Electronic publication date	March 2016
Version	1
Superseded publications	None
Review date	None
Author/s	JM Oduko, CJ Strudley, KC Young
Owner	NHS Breast Screening Programme
Document objective (clinical/healthcare/social questions covered)	To provide an evaluation of this equipment's suitability for use within the NHSBSP
Population affected	Women eligible for routine and higher-risk breast screening
Target audience	Physicists, radiographers, radiologists
Date archived	Current

Contents

Executive summary

The Siemens Inspiration with VB30L software, with or without the 'PRIME' option, was found to meet the main standards in the NHS Breast Screening Programme (NHSBSP) and European protocols. Performance data for comparison against other systems are provided in the report.

At the normal AEC dose setting the minimum acceptable standard of image quality was met for all breast thicknesses. For NHSBSP use it is recommended that the AEC dose be increased for thicknesses exceeding 60mm, in order to reach the achievable standard of image quality. Use of PRIME had no significant effect on image quality at a given dose level, but when segmentation was on, it reduced the dose for smaller breasts (which would lower the image quality).

1. Introduction

1.1 Testing procedures and performance standards for digital mammography

This report is one of a series evaluating commercially available direct digital radiography (DR) systems for mammography on behalf of the NHS Breast Screening Programme (NHSBSP). The testing methods and standards applied are mainly derived from NHSBSP Equipment Report 0604[1] and referred to in this document as 'the NHSBSP protocol'. The standards for image quality and dose are the same as those provided in the European protocol,[2,3] but the latter has been followed where it provides a more detailed performance standard, for example, for the automatic exposure control (AEC) system.

1.2 Objectives

The aims of the evaluation were:

- to determine whether the Siemens Inspiration with VB30L software, with or without the PRIME option, meets the main standards in the NHSBSP and European protocols

- to provide performance data for comparison against other systems

- to develop new tests which would show how segmentation operates, and test the dose reduction due to PRIME in an appropriate manner

2. Methods

2.1 System tested

The tests were conducted at the Siemens Headquarters in Erlangen, on a new Siemens Mammomat Inspiration PRIME which was set up ready for clinical use. It is described in Table 1, and shown in Figure 1.

Table 1. System Description

Manufacturer	Siemens
Model	Inspiration PRIME
System serial number	4551
Target material	Tungsten*
Added filtration	50µm rhodium
Detector type	Amorphous selenium
Detector serial number	L23-00463
Pixel size	85µm (in detector plane)
Detector area	239.4mm x 304.6mm
Field sizes	177mm x 238mm, 238mm x 299mm
Pixel array	2082 x 2800, 2800 x 3518
Pixel value offset	50
Source to detector distance	655.5mm for W/Rh
Source to table distance	633mm
Automatic exposure control (AEC) modes	OPDOSE, segmentation on or off, five dose levels: normal and ±10 or 20%
System software version	VB30L
AWS software version	VB41A (SL65P66)\/ syngo VE33A SL75P85 VB41A SL65 PACK P66\Aws SW versions\Aws\ device\ versions

* The molybdenum target with molybdenum or rhodium filter was not used in this evaluation

The system tested was equipped with the PRIME (Progressive Reconstruction Intelligently Minimising Exposure) option, which may be used for breast thicknesses up to 70mm. Instead of the system using a grid, the software identifies structures in the breast that cause scatter, and subtracts the calculated scatter. The mAs is lower when PRIME is in operation, as the X-rays are not absorbed by a grid. The dose saving depends on breast thickness but is typically 20%.

PRIME may be selected or deselected at the acquisition workstation. When the AEC is not in use, as in manual exposures for physics tests, these modes are more accurately

described as 'grid mode' (with PRIME off) or 'gridless mode' (with PRIME on). The scatter correction for the gridless mode is similar to that described above for breasts. The AEC system has 5 dose settings: low, medium low, normal, medium high and high. These allow selection of dose levels 10% or 20% above or below normal dose.

Figure 1. Inspiration PRIME

The AEC is a 'smart' system which identifies a denser region in the breast, a process known as segmentation. The system uses this denser region to select the appropriate exposure factors. If the tube is angled for an oblique view, a triangular region at the chest wall, corresponding to the expected position of pectoral muscle, is excluded from the search for a dense area.

The VB30L software version has not previously been evaluated by NCCPM. The results reported here under 'without PRIME' and grid mode headings describe the performance of the system with VB30L software.

2.2   Output and half-value-layer (HVL)

The output and HVL were measured as described in the NHSBSP protocol, at intervals of 3kV. The tungsten/rhodium target/filter combination was used for all measurements during the evaluation.

2.3   Detector response

The detector response was measured as described in the NHSBSP protocol, but with a different attenuator. The attenuator used was 2mm of aluminium placed at the tube exit port. An ion chamber was positioned above the table, 40mm from the chest wall edge (CWE). The incident air kerma was measured at the detector surface for a range of manually set mAs values at 29kV. The readings were corrected to the surface of the detector using the inverse square law. No correction was made for attenuation by the table and detector cover. Images acquired at the same mAs values were saved as unprocessed files. They were transferred to another computer for analysis. A 10mm square region of interest (ROI) was positioned on the midline, 40mm from the CWE of each image. The average pixel value and the standard deviation of pixel values within that region were measured. The relationship between average pixel values and the detector entrance surface air kerma was determined.

2.4   Dose measurement

Doses were measured using the X-ray set's AEC to expose different thicknesses of Perspex (polymethylmethacrylate or PMMA). Each block had an area of 180mm x 240mm. Spacers were used to adjust the paddle height to be equal to the equivalent breast thickness, as shown in Table 3. The exposure factors were noted and mean glandular doses (MGDs) were calculated for the equivalent breast thicknesses.

The measurements were made in grid mode at the normal dose setting and repeated in gridless mode, with segmentation off. (Further measurements made with segmentation on are described in Section 2.7). Some additional exposures were made at the low, medium low, medium high and high dose settings (in gridless mode and with segmentation off).

An aluminium square was used with the PMMA during these exposures, so that the images produced could be used for the calculation of contrast-to-noise ratio (CNR), in Section 2.5. The aluminium square, 10mm x 10mm and 0.2mm thick, was placed on top of a 20mm thick block, with one edge on the midline, 60mm from the chest wall edge. Additional layers of PMMA were placed on top of these to vary the total thickness.

2.5   Contrast-to-noise ratio (CNR)

Unprocessed images acquired during the dose measurement were downloaded and analysed to obtain the CNRs. Twenty small square ROIs (approximately 2.5mm x 2.5mm) were used to determine the average signal and the standard deviation in the signal within the image of the aluminium square (4 ROIs) and the surrounding background (16 ROIs), as shown in Figure 2. Small ROIs are used to minimise distortions due to the heel effect and other causes of non-uniformity.[4] However, because a flat-field correction is applied, this is less important for DR systems than in computed radiography systems. The CNR was calculated for each image, as defined in the NHSBSP and European protocols.
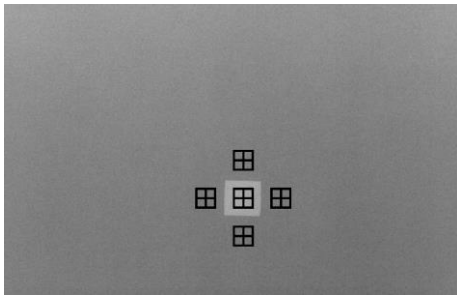

Figure 2. Location and size of ROI used to determine the CNR

To apply the standards in the European protocol, it is necessary to relate the image quality measured using the CDMAM (Section 2.8) for an equivalent breast thickness of 60mm, to that for other breast thicknesses. The European protocol gives the relationship between threshold contrast and CNR measurements, enabling the calculation of a target CNR value for a particular level of image quality. This can be compared to CNR measurements made at other breast thicknesses. Contrast for a particular gold thickness is calculated using Equation 1, and target CNR is calculated using Equation 2.

$$\text{Contrast} = 1 - e^{-\mu t} \tag{1}$$

where μ is the effective attenuation coefficient for gold, and t is the gold thickness.

$$\text{CNR}_{\text{target}} = \frac{\text{CNR}_{\text{measured}} \times \text{TC}_{\text{measured}}}{\text{TC}_{\text{target}}} \tag{2}$$

where $\text{CNR}_{\text{measured}}$ is the CNR for a 60mm equivalent breast, $\text{TC}_{\text{measured}}$ is the threshold contrast calculated using the threshold gold thickness for a 0.1mm diameter detail, (measured using the CDMAM at the same dose as used for $\text{CNR}_{\text{measured}}$), and $\text{TC}_{\text{target}}$ is the calculated threshold contrast corresponding to the threshold gold thickness required to meet either the minimum acceptable or achievable level of image quality as defined in the UK standard.

The 0.1mm detail threshold gold thickness is used here because it is generally regarded as the most critical of the detail diameters for which performance standards are set.

The effective attenuation coefficient for gold used in Equation 1 depends on the beam quality used for the exposure, and was selected from a table of values summarised in Table 2. These values were calculated with 3mm PMMA representing the compression paddle, using spectra from Boone et al.[5] and attenuation coefficients for materials in the test objects (aluminium, gold, PMMA) from Berger et al.[6]

Table 2. Effective attenuation coefficients for gold contrast details in the CDMAM

kV	target/filter	Effective attenuation coefficient (μm^{-1})
28	W/Rh	0.134
31	W/Rh	0.122
34	W/Rh	0.109

The European protocol also defines a limiting value for CNR, which is calculated as a percentage of the threshold contrast for minimum acceptable image quality for each thickness. This limiting value varies with thickness, as shown in Table 3.

Table 3. Limiting values for relative CNR

Thickness of PMMA (mm)	Equivalent breast thickness (mm)	Limiting values for relative CNR (%) in European protocol
20	21	> 115
30	32	> 110
40	45	> 105
45	53	> 103
50	60	> 100
60	75	> 95
70	90	> 90

The target CNR values for minimum acceptable and achievable levels of image quality and European limiting values for CNR were calculated. These were compared with the measured CNR results for all breast thicknesses in Section 3.3.2.

2.6   AEC performance for local dense areas

The local dense area test was used to evaluate the performance of the AEC operating in grid mode (without PRIME). A modified version of the test was developed to demonstrate the dose saving effect of operating the system with PRIME. Local dense areas were also used to demonstrate the exclusion of the pectoral muscle from the dense area selected when the tube is angled for oblique views.

2.6.1 Grid mode (without PRIME)

This test is described in the supplement to the fourth edition of the European protocol.[3] To simulate local dense areas, images were acquired under AEC (with segmentation on) of a 30mm thick block of PMMA (size 180mm x 240mm). Extra thicknesses of PMMA (20mm x 40mm in size, 2-10mm thick) were added to provide extra attenuation. The compression plate remained in position at 40mm height, as shown in Figure 3. The simulated dense area was positioned 50mm from the CWE of the table.

In the simulated local dense areas the mean pixel values and standard deviation for 10mm x 10mm ROIs were measured and the signal-to-noise ratios (SNRs) were calculated.
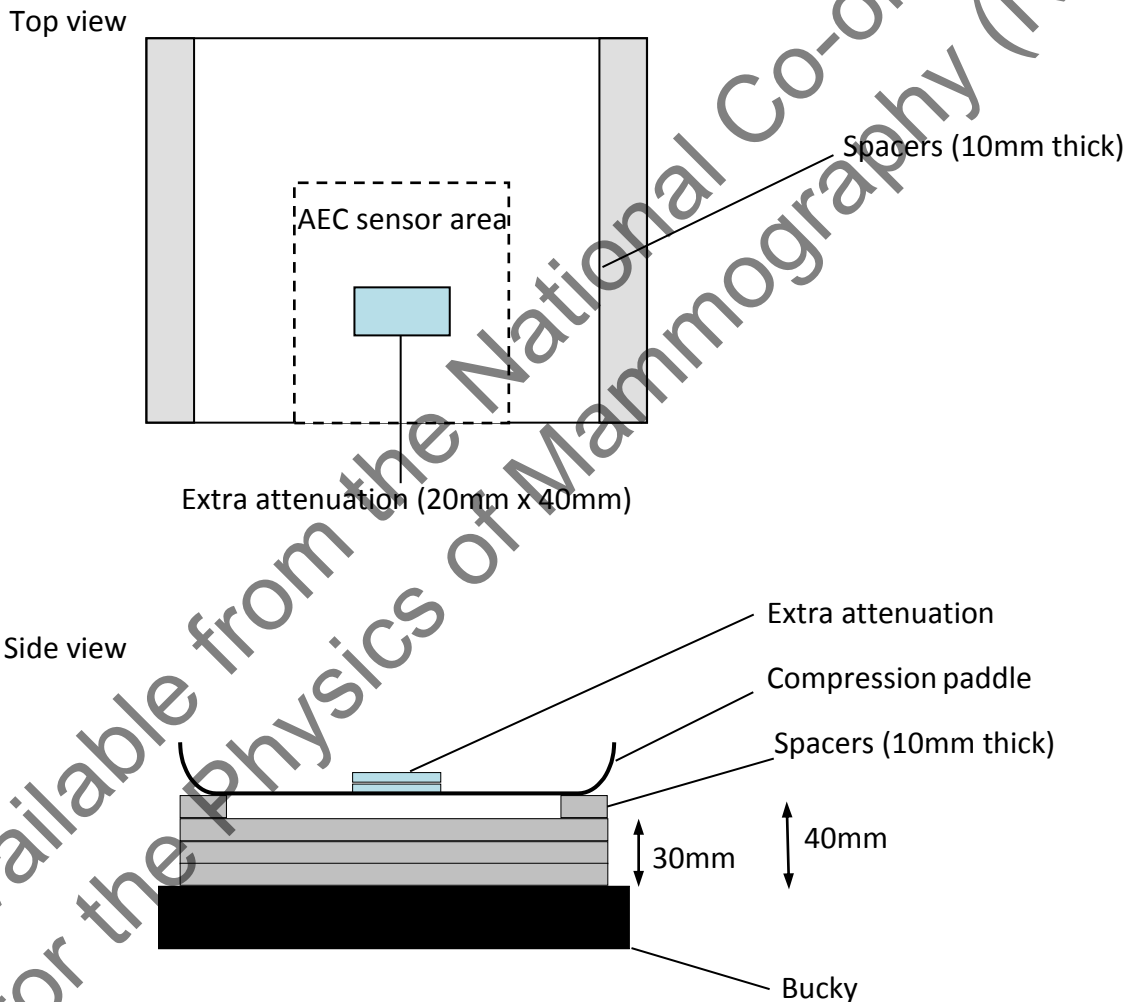

Figure 3. Setup to measure AEC performance for local dense areas

12

2.6.2 Test developed for PRIME with segmentation

PRIME is designed to operate when segmentation is turned on and a local dense area is detected, which the AEC uses to determine the exposure. The test described in Section 2.6.1 was modified to demonstrate more clearly, and measure, the dose saving when PRIME is used and a denser breast region is detected.

PMMA blocks of thickness 20 to 50mm were used, with the thickness of the small area of extra attenuation equal to one fifth of the PMMA block thickness. The paddle height was adjusted to that corresponding to the equivalent breast thickness for each PMMA block thickness. Exposures were made with segmentation on, both with and without PRIME. The mean pixel value and SNR in the area of extra attenuation were measured, and MGDs were calculated.

2.6.3 Demonstration of segmentation

A 50mm thickness of D-shaped PMMA (240mm x 120mm) was exposed under AEC control, with local dense areas simulated by either small thicknesses of 20mm x 40mm PMMA or a 0.3mm thickness of 100mm x 100mm aluminium foil. Images were acquired in grid mode, with segmentation on, with the tube in position as for clinical exposures: at the zero degree position as for clinical cranio-caudal views and at an angle of 28⁰ for mediolateral oblique views. Screenshots were taken of the images displayed on the acquisition workstation, showing the regions selected by the AEC to determine the exposure.

2.7 Noise analysis

The images acquired in the measurements of detector response, using 29kV W / Rh, were used to analyse the image noise. Small ROIs with an area of approximately 2.5mm x 2.5mm were placed on the midline, 60mm from the CWE. The average standard deviations of the pixel values in these ROIs for each image were used to investigate the relationship between the dose to the detector and the image noise. It was assumed that this noise comprises 3 components: electronic noise, structural noise, and quantum noise. The relationship between them is shown in Equation 3:

$$\sigma_p = \sqrt{k_e^2 + k_q^2 p + k_s^2 p^2} \qquad\qquad (3)$$

where σ_p is the standard deviation in pixel values within a ROI with a uniform exposure and a mean pixel value p, and k_e, k_q, and k_s are the coefficients determining the amount of electronic, quantum, and structural noise in a pixel with a value p. This method of analysis has been described previously.[7] For simplicity, the noise is generally presented here as relative noise defined as in Equation 4.

$$\text{Relative noise} = \frac{\sigma_p}{p} \tag{4}$$

The variation in relative noise with mean pixel value was evaluated and fitted using Equation 3, and non-linear regression used to determine the best fit for the constants and their asymptotic confidence limits (using Graphpad Prism Version 4.03 for Windows, Graphpad software, San Diego, California, USA, www.graphpad.com.). This established whether the experimental measurements of the noise fitted this equation, and the relative proportions of the different noise components. The relationship between noise and pixel values has been found empirically to be approximated by a simple power relationship as shown in Equation 5.

$$\frac{\sigma_p}{p} = k_t p^{-n} \tag{5}$$

where k_t is a constant. If the noise were purely quantum noise the value of n would be 0.5. However, the presence of electronic and structural noise means that n can be slightly higher or lower than 0.5.

The variance in pixel values within a ROI is defined as the standard deviation squared. The total variance was plotted against incident air kerma at the detector and fitted using Equation 3. Non-linear regression was used to determine the best fit for the constants and their asymptotic confidence limits, using the Graphpad Prism software.

Using the calculated constants the structural, electronic, and quantum components of the variance were estimated, assuming that each component was independently related to incident air kerma. The percentage of the total variance represented by each component was then calculated and plotted against incident air kerma at the detector.

2.8   Image quality measurements

Contrast detail measurements were made using a CDMAM phantom (serial number 1022, version 3.4, UMC St. Radboud, Nijmegen University, Netherlands). The phantom was positioned with a 20mm thickness of PMMA above and below, to give a total attenuation approximately equivalent to 50mm of PMMA or 60mm thickness of typical breast tissue. The kV and mAs were chosen to match as closely as possible that selected by the AEC when imaging a 50mm thickness of PMMA. This procedure was repeated to obtain a representative sample of 16 images at this dose level. The unprocessed images were transferred to disk for subsequent analysis off-site. Further images of the test phantom were then obtained at 0.5, 0.75, 1.5 and 2 times the AEC-selected dose, by manually selecting higher and lower mAs values with the same beam quality. Sets of images were obtained both in grid mode and with the anti-scatter grid removed and scatter correction applied.

An automatic method of reading the CDMAM images was used.[7, 8] Version 1.6 of CDCOM was used in the analysis. For each detail size the threshold gold contrast for a typical human observer was predicted using Equation 6.

$$TC_{predicted} = rTC_{auto}$$ (6)

where $TC_{predicted}$ is the predicted threshold contrast for a typical observer and TC_{auto} is the threshold contrast measured using an automated procedure with CDMAM images. r is the average ratio between human and automatic threshold contrast, determined experimentally, with the values shown in Table 4.

The contrasts used in Equation 6 were calculated from gold thickness using the effective attenuation coefficients shown in Table 2.

The main advantage of automatic reading is that it has the potential for eliminating observer error, which is a significant problem when using human observers.

The predicted threshold gold thickness for each detail diameter in the range 0.1mm to 1.0mm was fitted with a curve for each dose level, using the relationship shown in Equation 7.

$$Threshold\ gold\ thickness = a + bx^{-1} + cx^{-2} + dx^{-3}$$ (7)

where x is the detail diameter, and a, b, c and d are coefficients adjusted to obtain a least squares fit.

Table 4. Values of r used to predict threshold contrast

Diameter of gold disc (mm)	Average ratio of human to automatically measured threshold contrast (r)
0.08	1.40
0.10	1.50
0.13	1.60
0.16	1.68
0.20	1.75
0.25	1.82
0.31	1.88
0.40	1.94
0.50	1.98
0.63	2.01
0.80	2.06
1.00	2.11

15

The confidence limits for the predicted threshold gold thicknesses have been previously determined[7] by a re-sampling method, using a large set of images. The threshold contrasts quoted in the tables of results are derived from the fitted curves, as this has been found to improve accuracy.

The expected relationship between threshold contrast and dose is shown in Equation 8.

$$\text{Threshold contrast} = \lambda D^{-n} \qquad\qquad (8)$$

where D is the MGD for a 60mm thick standard breast (equivalent to the test phantom configuration used for the image quality measurement), and λ is a constant to be fitted.

It is assumed that a similar equation applies when using threshold gold thickness instead of contrast. This equation was plotted with the experimental data for each detail size from 0.1mm to 1.0mm. The value of n resulting in the best fit to the experimental data was determined, and the doses required for target CNR values were calculated for data relating to 0.1mm and 0.25mm detail diameters.

2.9   Physical measurements of detector performance

The modulation transfer function (MTF), normalised noise power spectrum (NNPS) and the detective quantum efficiency (DQE) of the system were measured. The methods used were as close as possible to those described by the International Electrotechnical Commission (IEC).[9] The radiation quality used for the measurements was adjusted by placing a uniform 2mm thick aluminium filter at the tube housing. The beam quality used was 29kV W/Rh. The test device to measure the MTF comprised a 0.8mm thick rectangle (120mm x 60mm) of stainless steel with polished straight edges. This test device was placed directly on the breast support table, and the grid was removed by selecting 'grid out' at the operator console. The test device was positioned to measure the MTF in 2 directions, first almost perpendicular and then almost parallel to the CWE.

To measure the noise power spectrum the test device was removed and exposures made for a range of incident air kerma at the surface of the table. The DQE is presented as the average of measurements in the directions perpendicular and parallel to the CWE.

3. Results

3.1 Output and HVL

The output and HVL measurements are shown in Table 5.

Table 5. Output and HVL

kV	target/filter	Output (µGy/mAs at 1m)	HVL (mm Al)
25	W/Rh	8.6	0.520
28	W/Rh	11.9	0.552
31	W/Rh	15.1	0.579
34	W/Rh	18.4	0.614

3.2 Detector response

The detector was found to have a linear response with an offset of 50 as shown in Figure 4.
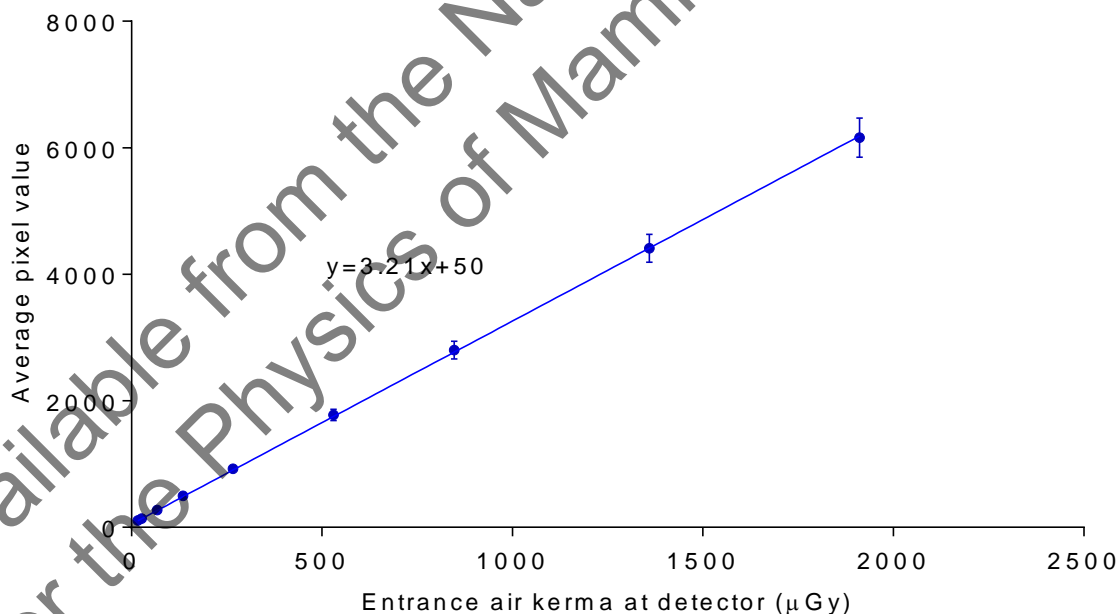

Figure 4. Detector response. (Error bars indicate 95% confidence limits.)

3.3 AEC performance

3.3.1 Dose

The MGDs for breasts simulated with PMMA exposed under AEC control are shown in Tables 6a and 6b for exposures made in grid mode and with PRIME respectively. These results were acquired with segmentation off, which is appropriate for physics measurements of uniform blocks.

Table 6a. MGD for simulated breasts (normal dose, grid in, segmentation off)

PMMA thickness (mm)	Equivalent breast thickness (mm)	kV	target/ filter	mAs	MGD (mGy)	NHSBSP remedial level (mGy)	AGD displayed (mGy)
20	21	26	W/Rh	30.8	0.41	> 1.0	0.50
30	32	27	W/Rh	45.5	0.55	> 1.5	0.63
40	45	28	W/Rh	67.8	0.77	> 2.0	0.82
45	53	29	W/Rh	77.4	0.90	> 2.5	0.92
50	60	30	W/Rh	86.9	1.05	> 3.0	1.01
60	75	31	W/Rh	123.8	1.44	> 4.5	1.33
70	90	32	W/Rh	174.7	1.94	> 6.5	1.79
80	107	32	W/Rh	266.5	2.58		2.40
85	116	32	W/Rh	356.9	3.16		3.01

Table 6b. MGD for simulated breasts (normal dose, PRIME, segmentation off)

PMMA thickness (mm)	Equivalent breast thickness (mm)	kV	target/ filter	mAs	MGD (mGy)	NHSBSP remedial level (mGy)	AGD displayed (mGy)
20	21	26	W/Rh	26.1	0.35	> 1.0	0.47
30	32	27	W/Rh	39.7	0.48	> 1.5	0.55
40	45	28	W/Rh	62.6	0.71	> 2.0	0.76
45	53	29	W/Rh	75.0	0.87	> 2.5	0.88
50	60	30	W/Rh	86.9	1.05	> 3.0	1.01

At all thicknesses the dose was below the remedial level in the NHSBSP protocol, which is the same as the maximum acceptable level in the European protocol. The displayed average glandular dose (AGD) values in Tables 6a and 6b are different from the MGD values presented here, which are calculated according to Dance et al.[10] The differences are small (<10%), except for the smallest thicknesses (21 and 32mm equivalent breast thickness).

The results presented in Tables 6a and 6b are also presented graphically in Figure 5, together with results obtained with segmentation on, and added dense areas, from Section 3.3.4.
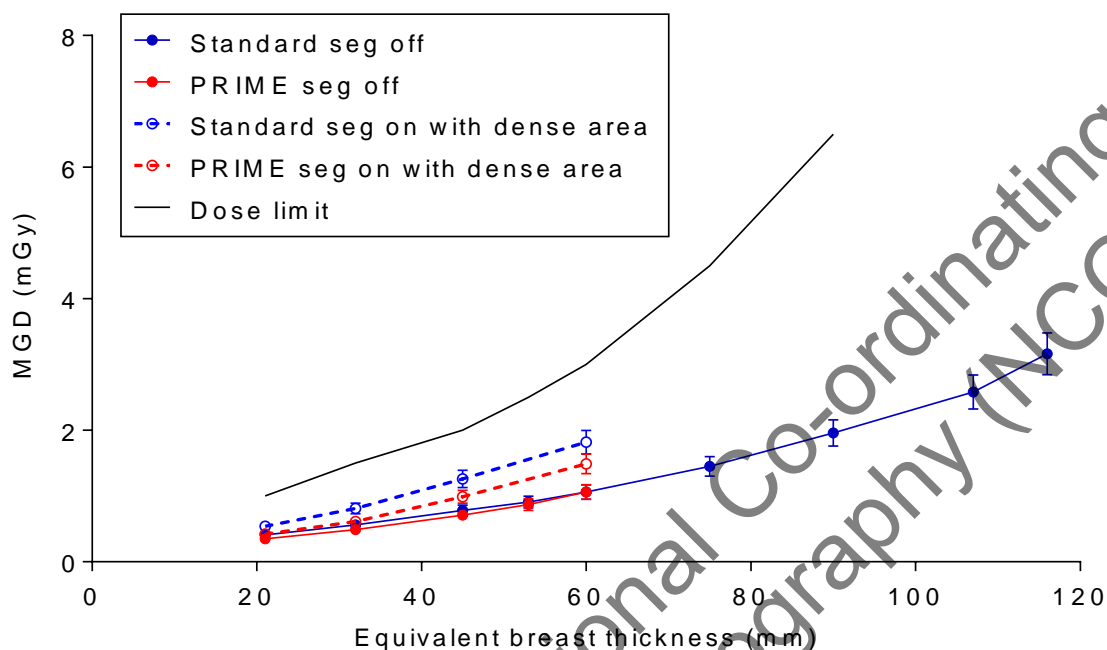

Figure 5. MGD for different thicknesses of simulated breasts, normal dose mode. (Error bars indicate 95% confidence limits.)

Results of the measurements at different dose settings are shown in Table 6c. The percentage differences measured are close to the nominal percentages supplied by Siemens.

Table 6c. MGD for simulated breasts at different doses (grid in, segmentation off)

AEC setting	PMMA thickness (mm)	kV	target/ filter	mAs	MGD (mGy)	% of normal dose	nominal % of normal dose
low	45	29	W/Rh	62.8	0.73	82	80
medium low	45	29	W/Rh	69.6	0.81	91	90
normal	45	29	W/Rh	76.8	0.89	100	100
medium high	45	29	W/Rh	84.6	0.98	110	110
high	45	29	W/Rh	91.0	1.06	118	120
high	20	26	W/Rh	35.9	0.48	117	120
high	70	32	W/Rh	201.6	2.24	115	120

19

3.3.2 CNR

The results of the CNR measurements for images acquired in grid mode and with PRIME are shown in Tables 7a, 7b respectively and in Figure 6. The CNRs required to meet the minimum acceptable and achievable image quality standards at the 60mm breast thickness were calculated. The CNRs required at each thickness to meet the limiting value for CNR in the European protocol were calculated and are also shown.

Table 7a. Contrast and CNR measurements for exposures made in grid mode

PMMA thickness (mm)	Equivalent breast thickness (mm)	Background pixel value	Measured CNR	CNR for minimum acceptable IQ	CNR for achievable IQ	European limiting CNR value
20	21	321	8.81	4.31	6.36	4.96
30	32	320	7.89	4.31	6.36	4.75
40	45	319	7.40	4.31	6.36	4.53
45	53	321	6.92	4.31	6.36	4.44
50	60	320	6.50	4.31	6.36	4.31
60	75	324	5.73	4.31	6.36	4.10
70	90	336	5.07	4.31	6.36	3.88
80	107	326	4.51	4.31	6.36	
85	116	345	4.53	4.31	6.36	

Table 7b. Contrast and CNR measurements for grid-less exposures with PRIME

PMMA thickness (mm)	Equivalent breast thickness (mm)	Background pixel value	Measured CNR	CNR for minimum acceptable IQ	CNR for achievable IQ	European limiting CNR value
20	21	335	8.38	4.31	6.36	4.96
30	32	344	7.65	4.31	6.36	4.74
40	45	356	6.96	4.31	6.36	4.53
45	53	366	6.71	4.31	6.36	4.44
50	60	370	6.20	4.31	6.36	4.31

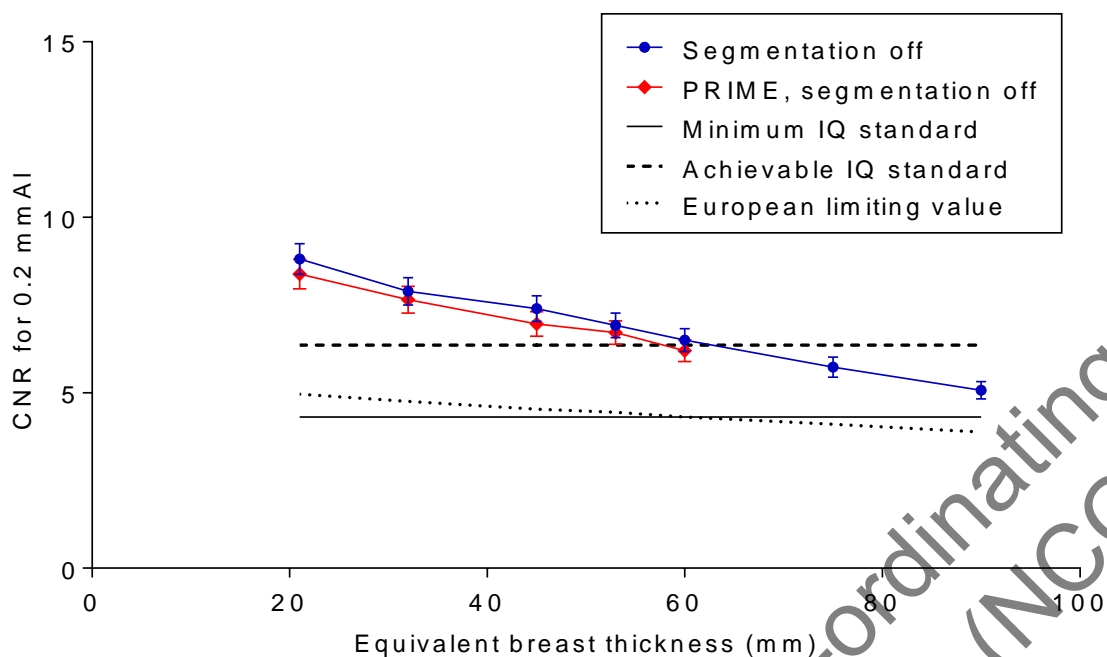Note: PRIME only operates for breast thicknesses up to 70mm.

Figure 6. Measured CNR compared with the limiting values in the European protocol. (Error bars indicate 95% confidence limits.)

3.3.3 AEC performance for local dense areas in grid mode (without PRIME)

In grid mode (without PRIME), it is expected that when the AEC adjusts for locally dense areas, the SNR will remain constant with increasing thickness of extra PMMA. The results presented in Table 8 and Figure 7 confirm this expectation and show that the SNR remains constant as thickness increases.

For attenuation greater than 40mm the AEC did not correctly select the locally dense area (as shown by visualising it), because the thicknesses prescribed in the test were unsuitable. A modified test was therefore developed, and is described in Section 3.3.4. Visualisation of the AEC-selected region is shown in Section 3.3.5.

Table 8. AEC performance for local dense areas

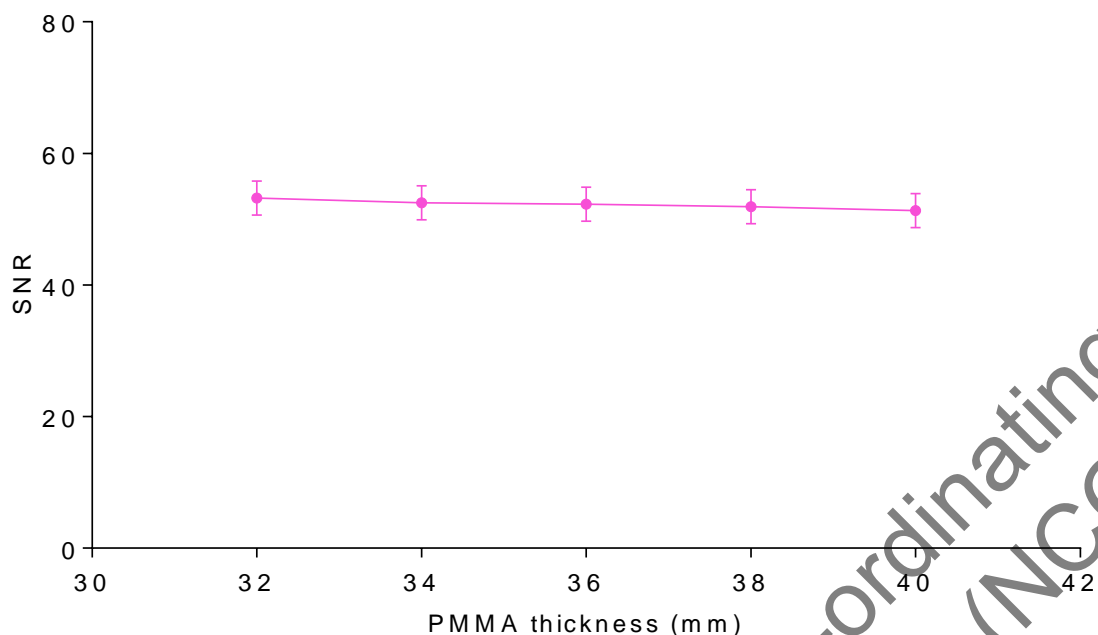| Total attenuation (mm PMMA)	kV	Target /filter	Tube load (mAs)	SNR	% difference from mean SNR
32	28	W/Rh	44.4	53.2	1.8
34	28	W/Rh	48.8	52.5	0.5
36	28	W/Rh	53.7	52.3	0.1
38	28	W/Rh	58.8	51.9	-0.6
40	28	W/Rh	63.1	51.3	-1.9

Figure 7. AEC performance for local dense areas. (Error bars indicate 95% confidence limits.)

3.3.4 Test developed for PRIME with segmentation

Increasing the extra PMMA thickness in proportion to the PMMA block thickness allowed PRIME to work in the manner intended, with segmentation on. (The results in Tables 6a and 6b, measured with uniform blocks, do not correctly indicate the performance of PRIME in clinical use, where a dense region of the breast is selected and used to determine exposure factors). The higher MGDs determined in this test are shown in Figure 5. The variation in the pixel value and SNR in the extra dense area are shown in Figures 8 and 9. There is a small decrease in pixel value and SNR with thickness when PRIME is used. All the MGDs (segmentation on and off, with and without PRIME) are compared in Table 9. The values for segmentation off are reproduced from Tables 6a and 6b, for comparison here.

Table 9. Calculated MGDs for segmentation on and off, with and without PRIME

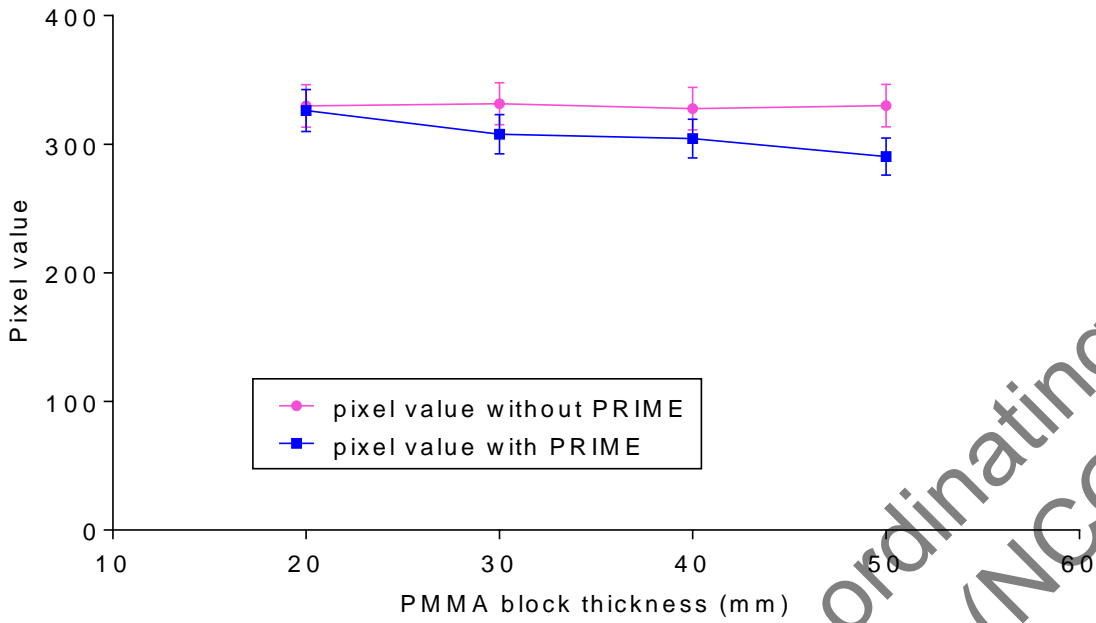| PMMA (mm)	Plain PMMA Segmentation off		With local dense area Segmentation on		
	MGD (mGy) without PRIME	MGD (mGy) with PRIME	Dense area (mm PMMA)	MGD (mGy) without PRIME	MGD (mGy) with PRIME
20	0.41	0.35	4	0.54	0.42
30	0.55	0.48	6	0.81	0.61
40	0.77	0.71	8	1.25	0.98
50	1.05	1.05	10	1.80	1.48

Figure 8. Mean pixel value in dense area, with and without PRIME. (Error bars indicate 95% confidence limits.)
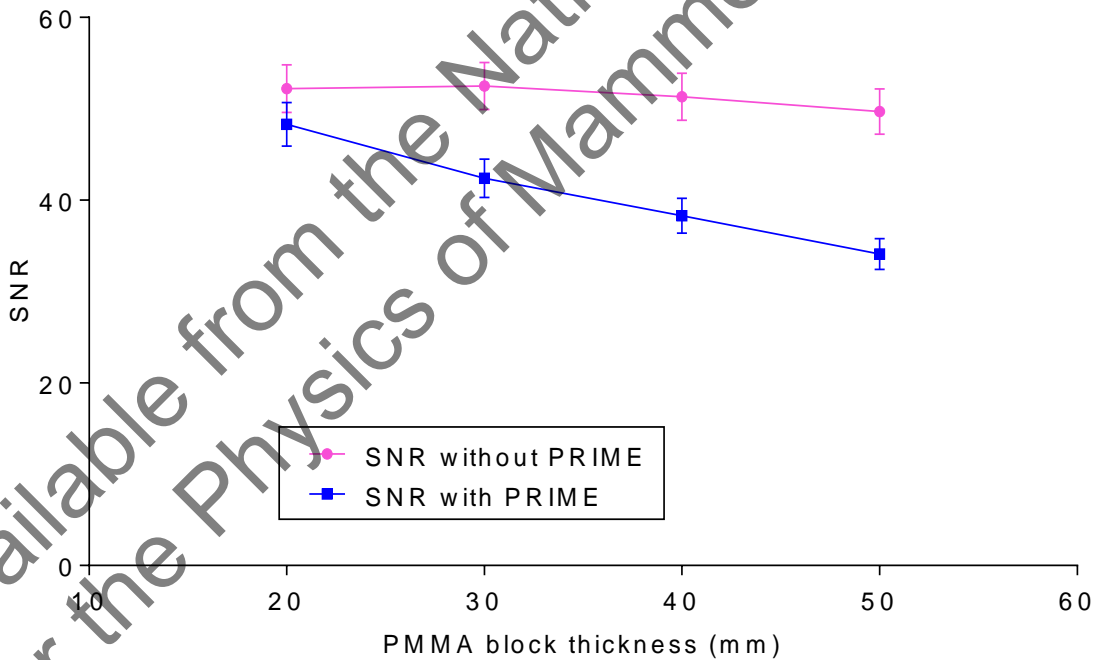

Figure 9. Mean SNR in dense area, with and without PRIME. (Error bars indicate 95% confidence limits.)

3.3.5 Demonstration of segmentation

When insufficient extra PMMA was added to D-shaped PMMA (for example 2mm extra of 20mm x 40mm PMMA added to 20mm thickness), the segmentation did not find the extra attenuation and outlined the whole 'breast', as shown in Figure 10. Greater extra thicknesses of extra PMMA were detected, as shown by the outline in Figure 13, and aluminium foil (0.1 to 0.3mm thick) was always detected (as shown in Figure 11).

Figures 10 and 11 were the results with the tube angle at 0°. When the tube was angled at -28°, as for an oblique view, the AEC did not detect any attenuating object inside a triangular region corresponding to the pectoral muscle, as shown in Figures 12, 13 and 14.

Outlines such as those in the screenshots shown in Figures 10 to14 can be displayed immediately after the acquisition of each image, but cannot be saved. Occasionally images in this series, like others acquired during the evaluation, were displayed with black-white inversion, as shown in Figure 10, but the pixel values were not affected when this occurred.
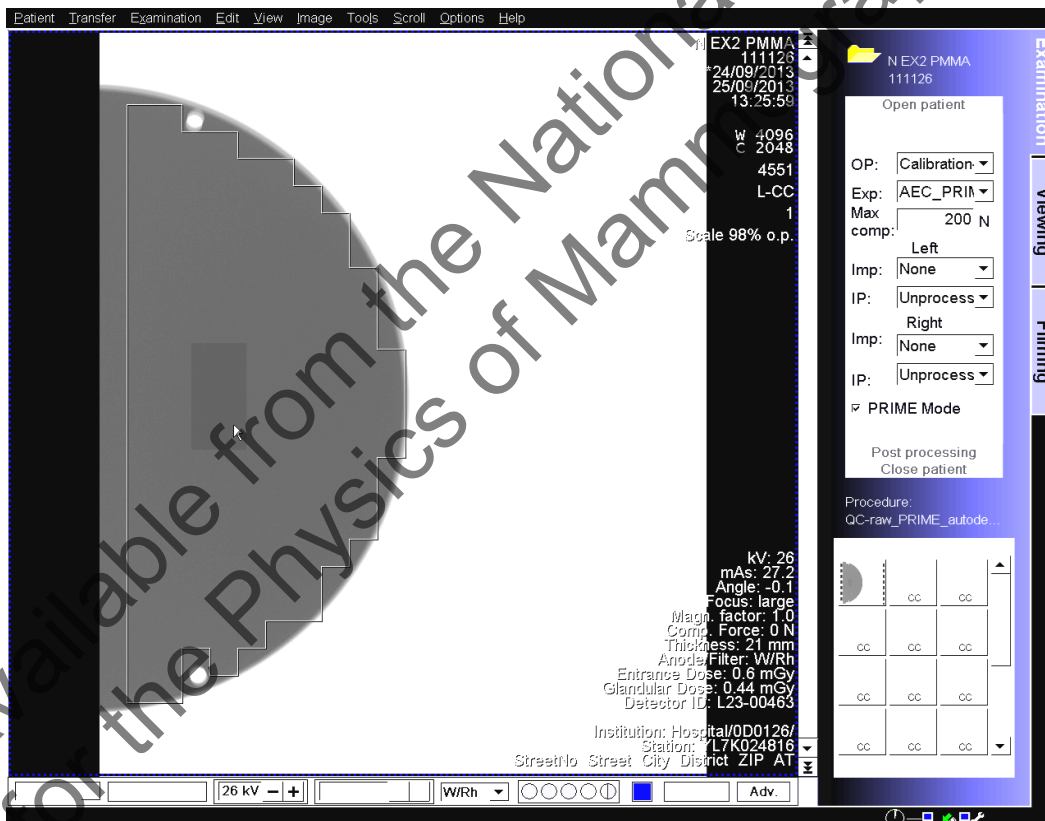

Figure 10. A very thin layer of PMMA is not detected and the whole 'breast' is selected by the AEC. (Tube angle 0°.)
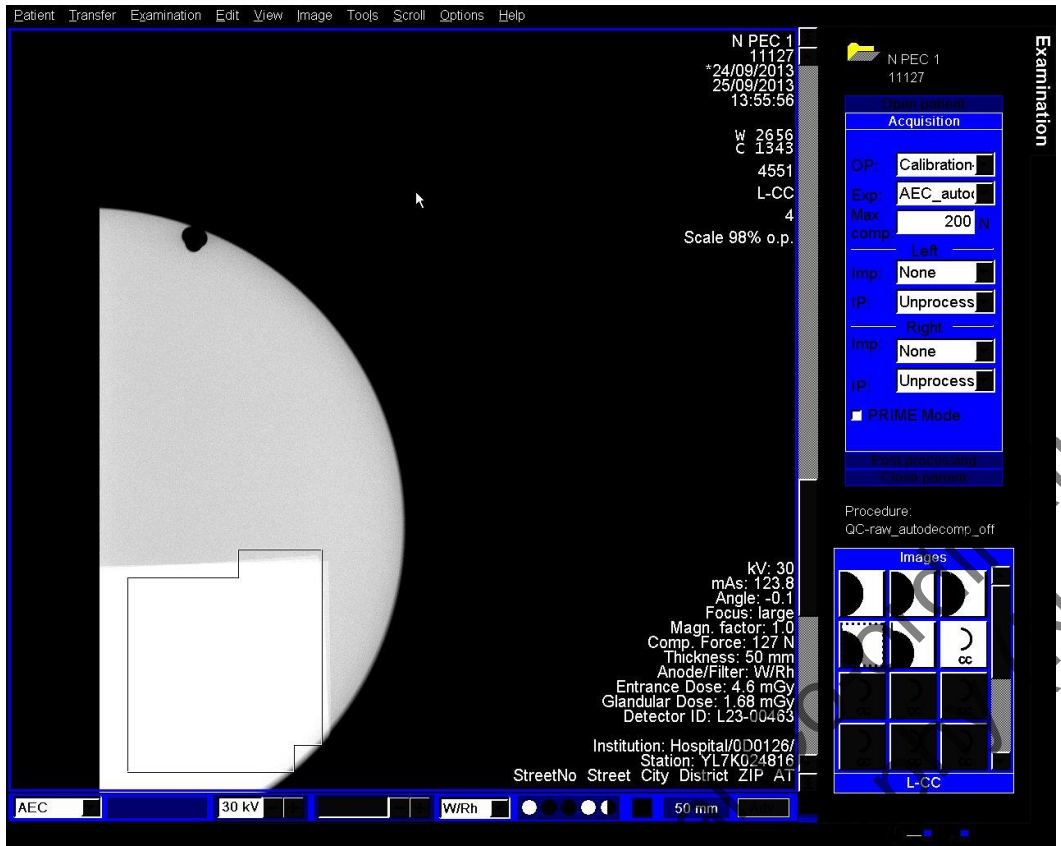
Figure 11. Aluminium foil is detected by the AEC. (Tube angle 0°.)

Figure 12. Aluminium foil is detected by the AEC outside the pectoral muscle region but not inside it. (Tube angle -28°.)
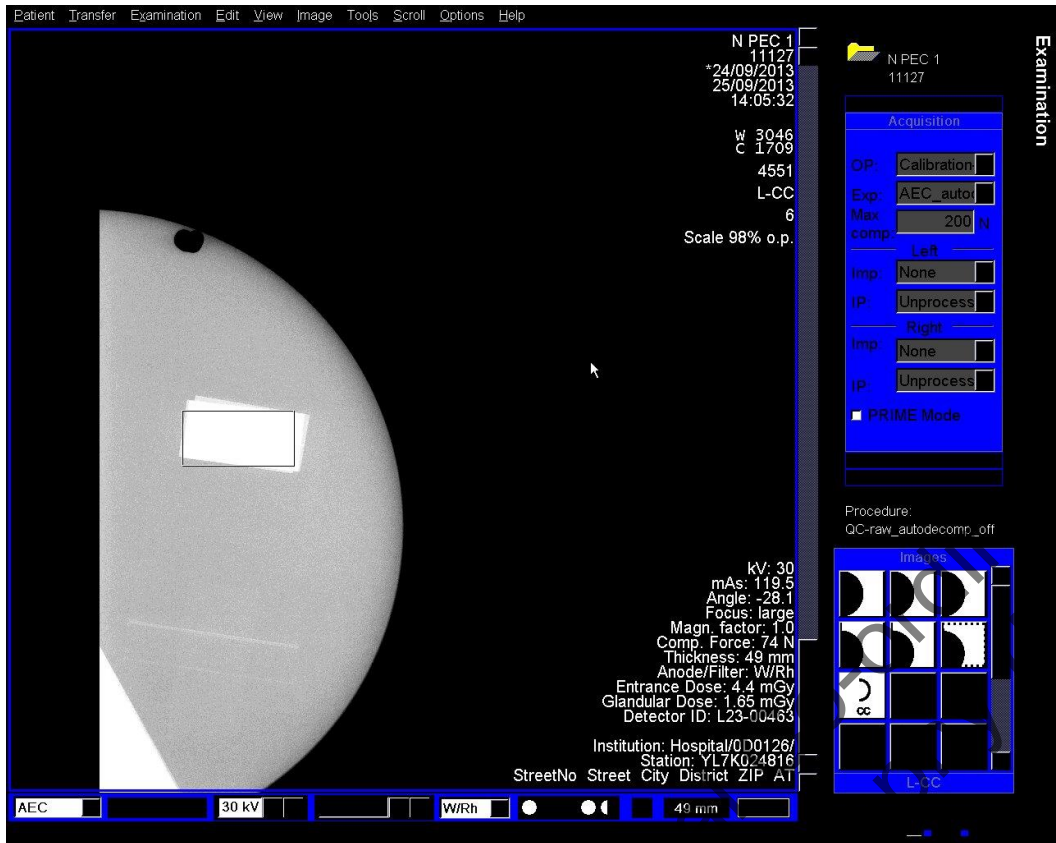
Figure 13. Sufficient thickness of PMMA is detected by the AEC, aluminium foil inside the pectoral muscle region is not detected. (Tube angle -28°.)
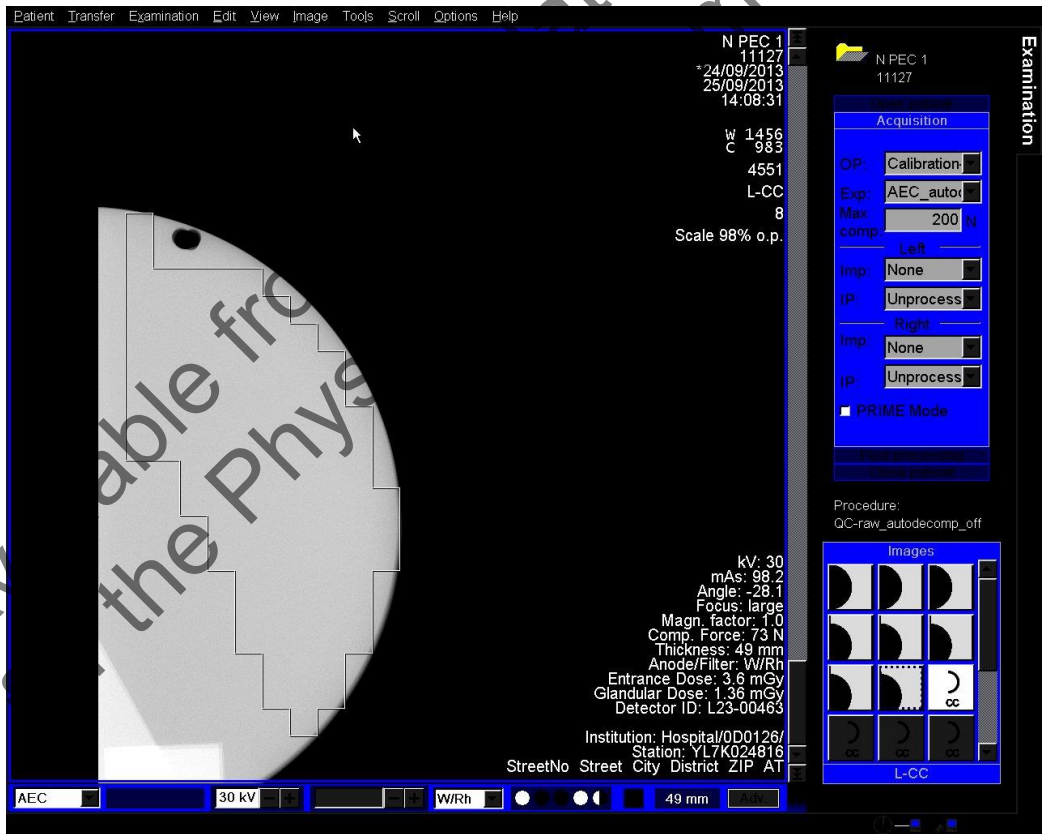

Figure 14. Aluminium foil and PMMA inside the pectoral muscle region are not detected by the AEC. (Tube angle -28°.)

3.4   Noise measurements

The variation in noise with dose was analysed by plotting the standard deviation in pixel values against the detector entrance air kerma, as shown in Figure 15. The fitted power curve has an index of 0.43, close to 0.50 which would be the expected value if quantum noise sources alone were present.

Figure 16 is an alternative way of presenting the data and shows the relative noise at different entrance air kerma. The estimated relative contributions of electronic, structural, and quantum noise are shown and the quadratic sum of these contributions fitted to the measured noise (using Equation 3).

Figure 17 shows the different amounts of variance due to each component, and the percentage quantum variance is seen in comparison to the 80% limit. The vertical dashed lines indicate the range of incident air kerma determined during AEC tests with different thicknesses of PMMA.
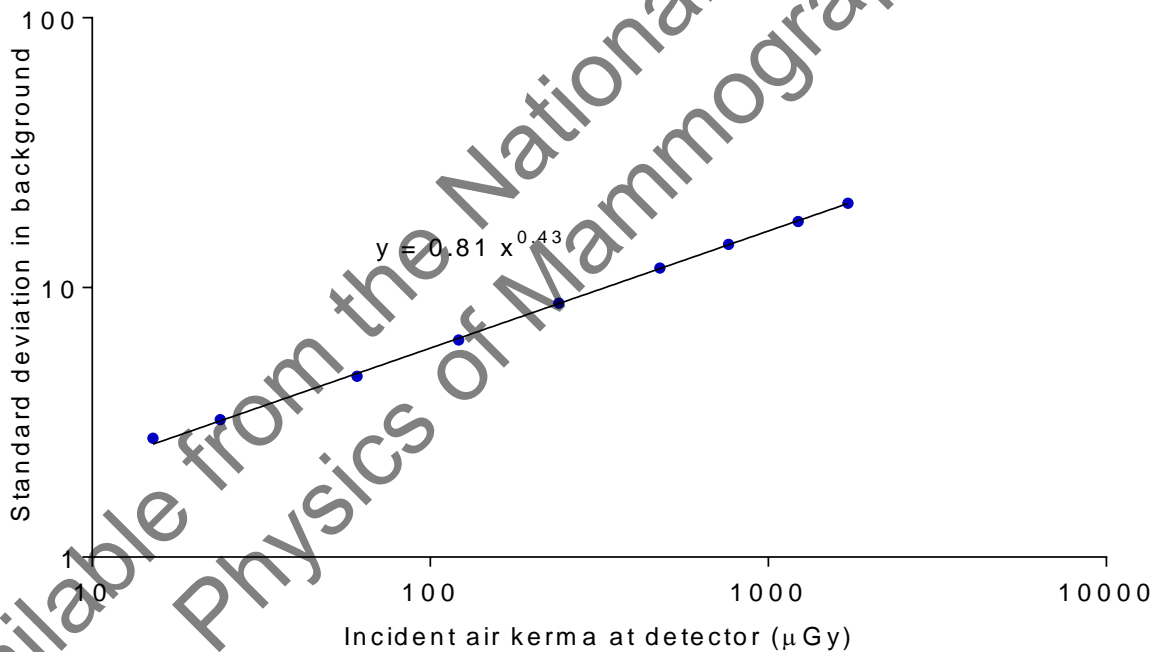

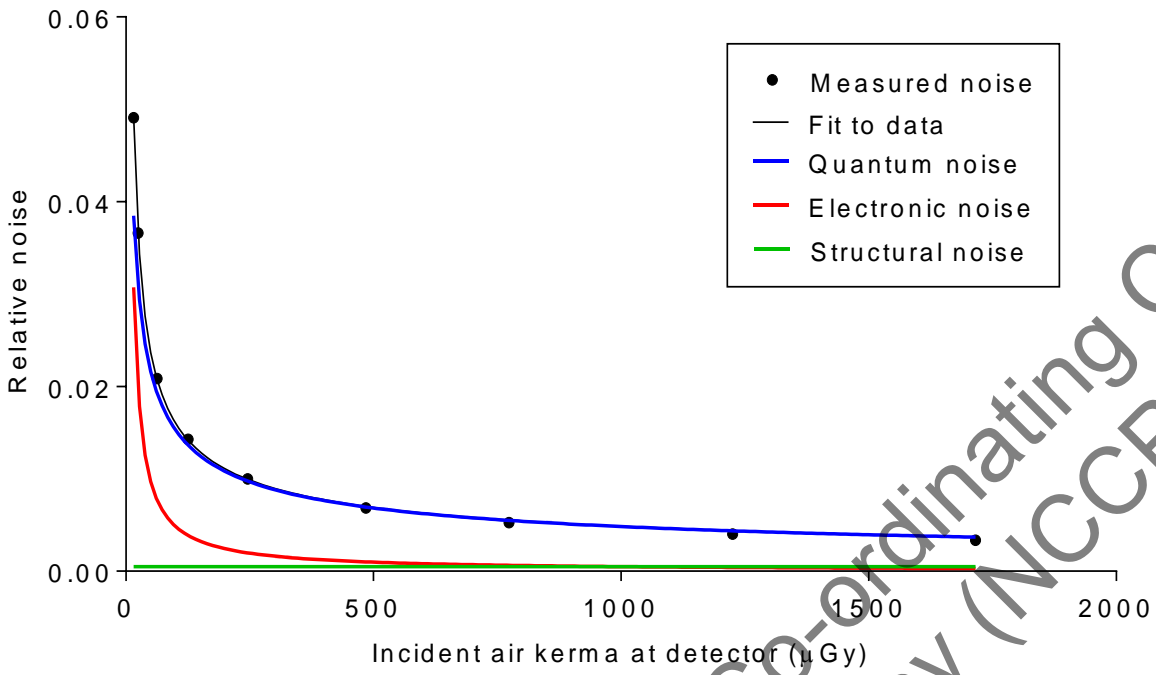**Figure 15. Standard deviation of pixel values versus air kerma at detector**

27

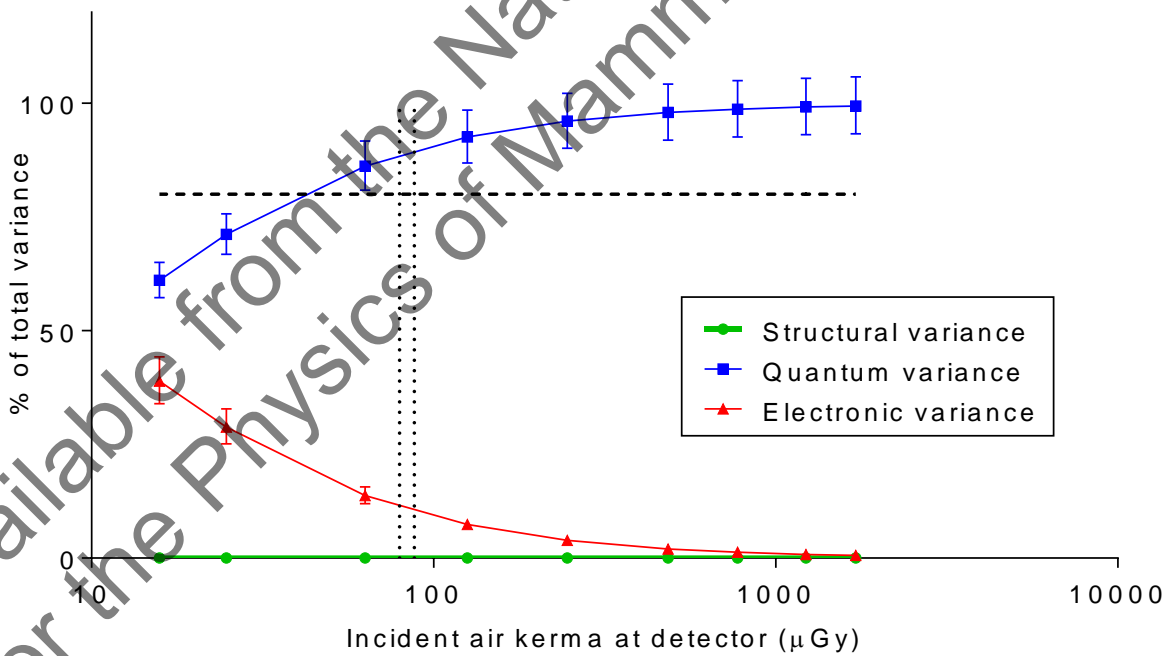**Figure 16. Relative noise and noise components**

Figure 17. Noise components as a percentage of the total variance. (Error bars indicate 95% confidence limits.)

3.5   Image quality measurements

The first exposure of the image quality phantom was made using the AEC at normal dose, grid in and segmentation off, to select the beam quality and exposure factors. This resulted in the selection of 30kV W/Rh, 90mAs. Subsequent image quality measurements were made by manual selection, at a range of mAs values between half and double the AEC-selected mAs at the same kV, as shown in Table 10. The corresponding MGDs to equivalent breasts (60mm thick) are also shown in Table 10.

Table 10. Images acquired for image quality measurement

kV	Target/filter	Tube loading (mAs)	Mean glandular dose to equivalent breasts 60mm thick (mGy)	Number of CDMAM images acquired and analysed
30	W/Rh	45	0.54	16
30	W/Rh	63	0.76	16
30	W/Rh	90	1.09	16
30	W/Rh	125	1.51	16
30	W/Rh	180	2.17	16

The contrast detail curves at the different dose levels (determined by automatic reading of the images) are shown in Figures 18a and 18b. The threshold gold thicknesses measured for different diameters at the 5 dose levels in grid mode and in grid-less mode with scatter correction applied (PRIME) are shown in Tables 11a and 11b, respectively. The NHSBSP minimum and achievable limits are also shown.
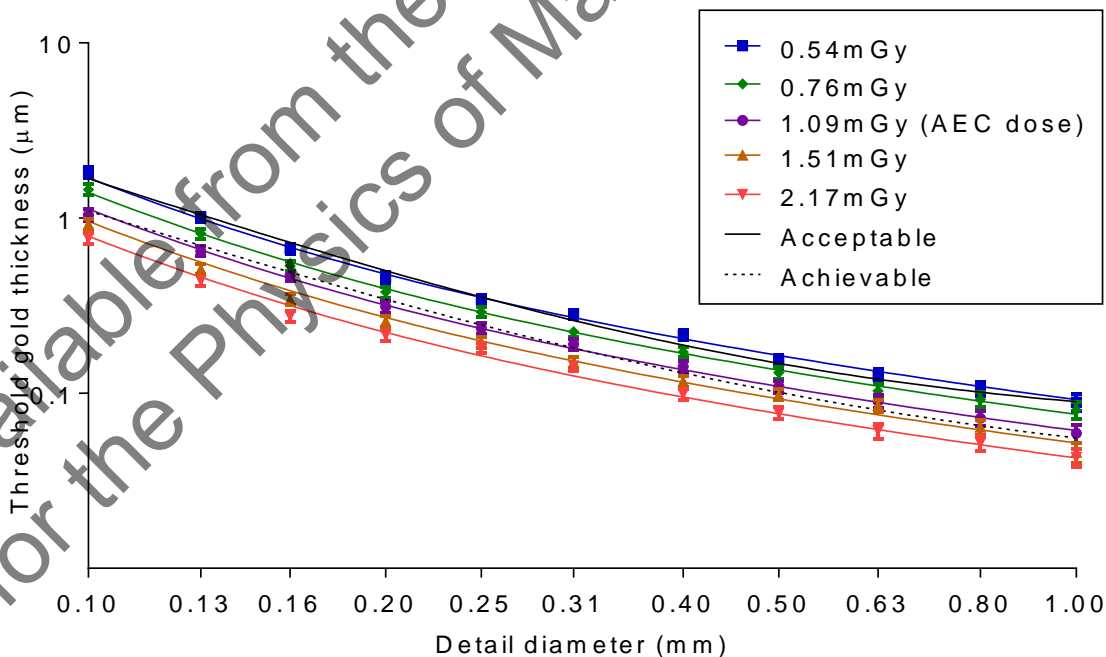

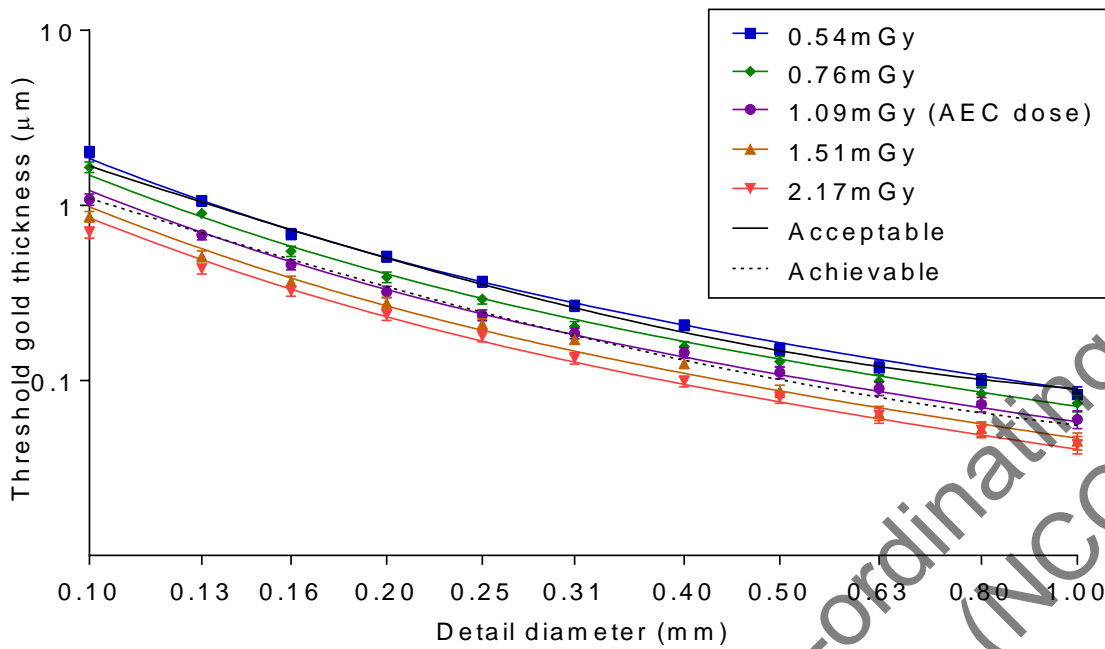**Figure 18a. Contrast-detail curves for 5 doses at 30kV W/Rh (grid mode). (Error bars indicate 95% confidence limits.)**

29

Figure 18b. Contrast-detail curves for 5 doses at 30kV W/Rh (grid-less scatter correction mode). (Error bars indicate 95% confidence limits.)

Table 11a. Fit to predicted human threshold gold thicknesses for different detail diameters for 5 doses using 30kV W/Rh (grid mode), and automatically predicted data

Diam-eter (mm)	Accept-able value	Achiev-able value	Threshold gold thickness (µm)				
			MGD = 0.54mGy	MGD = 0.76mGy	MGD = 1.09mGy	MGD = 1.51mGy	MGD = 2.17mGy
0.1	1.680	1.100	1.822 ± 0.130	1.453 ± 0.104	1.043 ± 0.077	0.922 ± 0.064	0.767 ± 0.053
0.25	0.352	0.244	0.340 ± 0.025	0.291 ± 0.020	0.235 ± 0.017	0.196 ± 0.014	0.181 ± 0.012
0.5	0.150	0.103	0.153 ± 0.013	0.131 ± 0.011	0.109 ± 0.009	0.098 ± 0.007	0.077 ± 0.006
1	0.091	0.056	0.089 ± 0.010	0.080 ± 0.009	0.059 ± 0.007	0.046 ± 0.006	0.043 ± 0.005

Table 11b. Average threshold gold thicknesses for different detail diameters for 5 doses using 30kV W/Rh (scatter correction mode), and automatically predicted data

Diam-eter (mm)	Accept-able value	Achiev-able value	Threshold gold thickness (µm)				
			MGD = 0.54mGy	MGD = 0.76mGy	MGD = 1.09mGy	MGD = 1.51mGy	MGD = 2.17mGy
0.1	1.680	1.100	2.023 ± 0.143	1.653 ± 0.114	1.081 ± 0.080	0.863 ± 0.059	0.702 ± 0.051
0.25	0.352	0.244	0.367 ± 0.026	0.292 ± 0.019	0.236 ± 0.017	0.210 ± 0.015	0.179 ± 0.013
0.5	0.150	0.103	0.151 ± 0.012	0.128 ± 0.009	0.111 ± 0.009	0.087 ± 0.007	0.080 ± 0.006
1	0.091	0.056	0.083 ± 0.009	0.074 ± 0.008	0.060 ± 0.007	0.045 ± 0.005	0.043 ± 0.005

The measured threshold gold thicknesses are plotted against the MGD for a 60mm thick equivalent breast, for the 0.1 and 0.25mm detail sizes, in Figure 19. The curves in Figure 19, which are of the form $y = x^{-n}$, were interpolated to find the doses required to meet the minimum acceptable and achievable threshold gold thicknesses, shown in Tables 12 and 13.
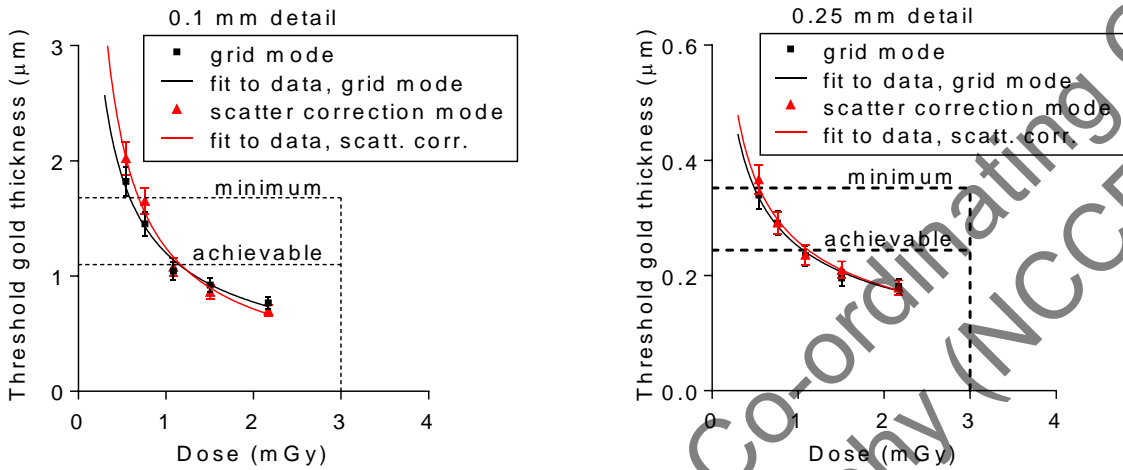

Figure 19. Threshold gold thickness at different doses. (Error bars indicate 95% confidence limits.)

3.6 Comparison with other systems

The MGDs to reach the minimum and achievable image quality standards in the NHSBSP protocol have been estimated from the curves shown in Figure 19. The fitted curves are of the form $y = x^{-n}$. (The error in estimating these doses depends on the accuracy of the curve fitting procedure, and pooled data for several systems has been used to estimate the 95% confidence limits of about 20%.) These doses are shown against similar data for other models of digital mammography system in Tables 12 and 13 and Figures 20 to 23. The data for the other systems has been determined in the same way as described in this report and the results published previously.[11-18] The data for film screens represent an average value determined using a variety of film screen systems which were in use recently.

Table 12. The MGD for a 60mm equivalent breast for different systems to reach the minimum threshold gold thickness for 0.1mm and 0.25mm details

System	MGD (mGy) for 0.1mm	MGD (mGy) for 0.25mm
Siemens Inspiration (grid-less with scatter correction)	**0.58 ± 0.12**	**0.59 ± 0.12**
Siemens Inspiration (grid mode)	**0.54 ± 0.11**	**0.55 ± 0.11**
Siemens Inspiration (previous report)[14]	0.76 ± 0.15	0.60 ± 0.12
Fuji Amulet f/s	0.79 ± 0.16	0.58 ± 0.12
GE Essential	0.49 ± 0.10	0.49 ± 0.10
Hologic Dimensions	0.34 ± 0.07	0.48 ± 0.10
Hologic Selenia (W)	0.71 ± 0.14	0.64 ± 0.13
IMS Giotto 3DL	0.93 ± 0.19	0.70 ± 0.14
Philips MicroDose L30 C120	0.67 ± 0.13	0.47 ± 0.09
Film-screen	1.30 ± 0.26	1.36 ± 0.27
Agfa CR (NIP)	1.27 ± 0.25	0.96 ± 0.19
Fuji Profect CR	1.78 ± 0.36	1.35 ± 0.27

Table 13. The MGD for a 60mm equivalent breast for different systems to reach the achievable threshold gold thickness for 0.1mm and 0.25mm details

| System	MGD (mGy) for 0.1mm	MGD (mGy) for 0.25mm
Siemens Inspiration (grid-less with scatter correction)	**1.22 ± 0.24**	**1.12 ± 0.22**
Siemens Inspiration (grid mode)	**1.16 ± 0.23**	**1.06 ± 0.21**
Siemens Inspiration (previous report)[14]	1.27 ± 0.25	1.16 ± 0.23
Fuji Amulet f/s	1.35 ± 0.27	1.58 ± 0.32
GE Essential	1.13 ± 0.23	1.03 ± 0.21
Hologic Dimensions	0.87 ± 0.17	1.10 ± 0.22
Hologic Selenia (W)	1.37 ± 0.27	1.48 ± 0.30
IMS Giotto 3DL	1.60 ± 0.32	1.41 ± 0.28
Philips MicroDose L30 C120	1.34 ± 0.27	1.06 ± 0.21
Film-screen	3.03 ± 0.61	2.83 ± 0.57
Agfa CR (NIP)	2.47 ± 0.49	2.34 ± 0.47
Fuji Profect CR	3.29 ± 0.66	2.65 ± 0.53
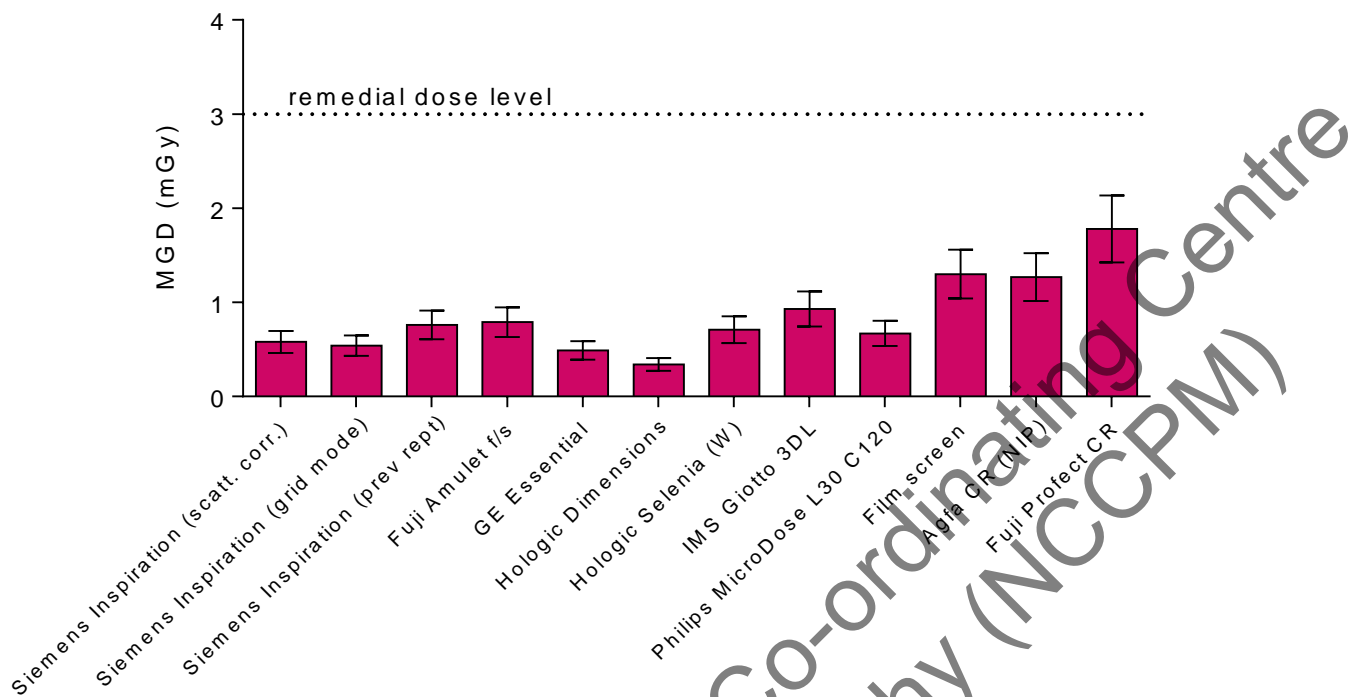
Figure 20. MGD for a 60mm equivalent breast to reach minimum acceptable image quality standard for 0.1mm detail. (Error bars indicate 95% confidence limits.)
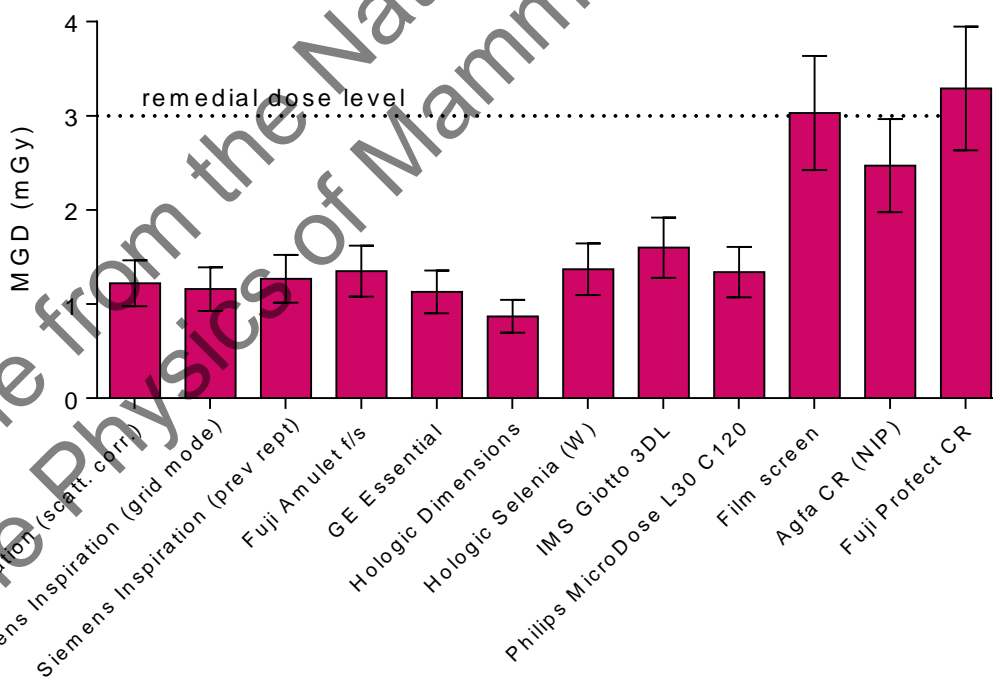

Figure 21. MGD for a 60mm equivalent breast to reach achievable image quality standard for 0.1mm detail. (Error bars indicate 95% confidence limits.)
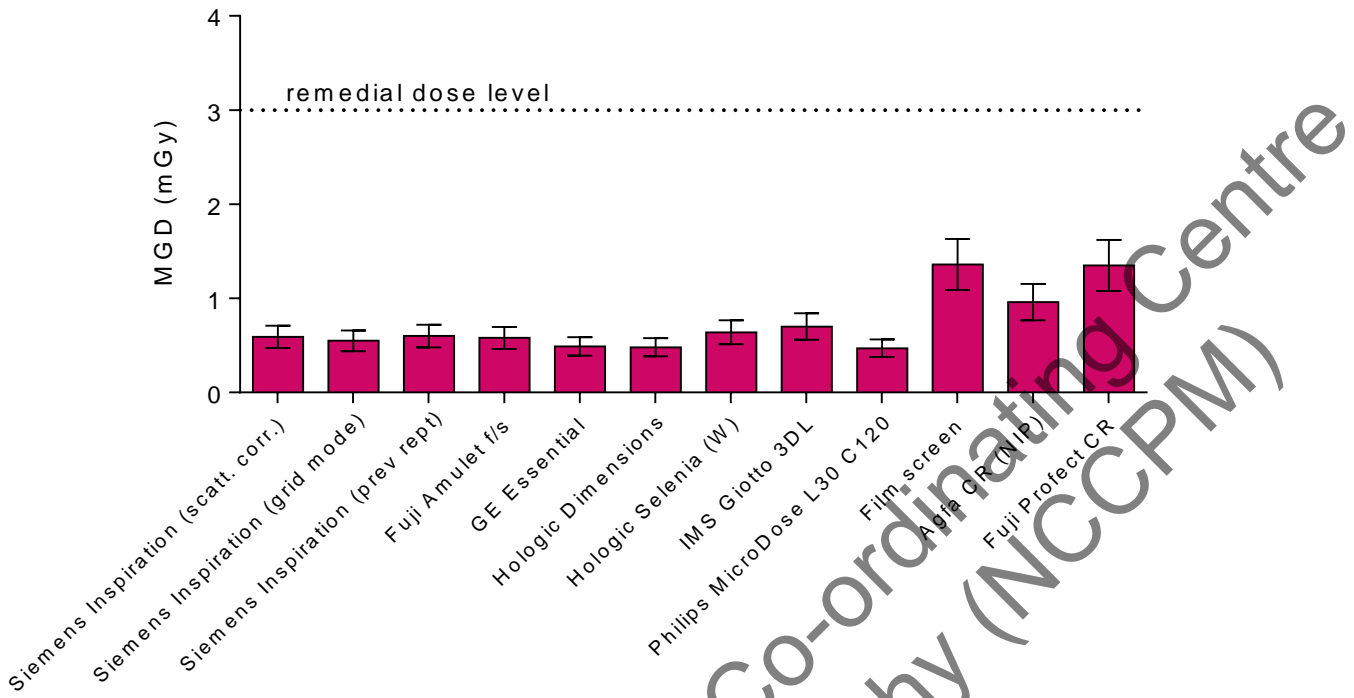
33

Figure 22. MGD for a 60mm equivalent breast to reach minimum acceptable image quality standard for 0.25mm detail. (Error bars indicate 95% confidence limits.)
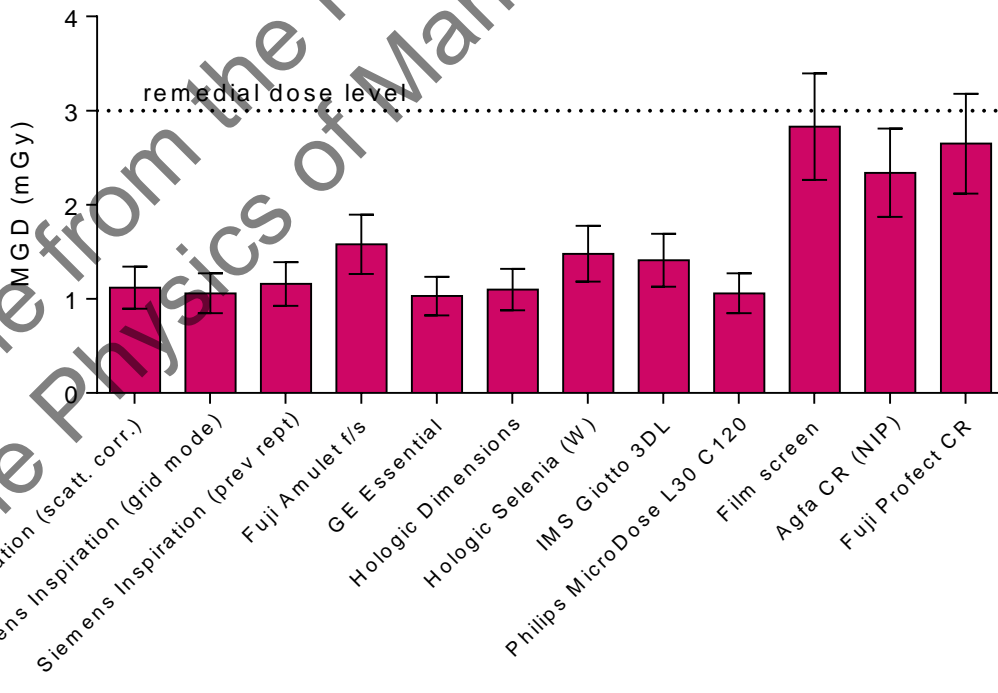

Figure 23. MGD for a 60mm equivalent breast to reach achievable image quality standard for 0.25mm detail. (Error bars indicate 95% confidence limits.)

3.7   Detector performance

The MTF is shown in Figure 24 for the 2 orthogonal directions. Figure 25 shows the NNPS curves for a range of entrance air kerma.
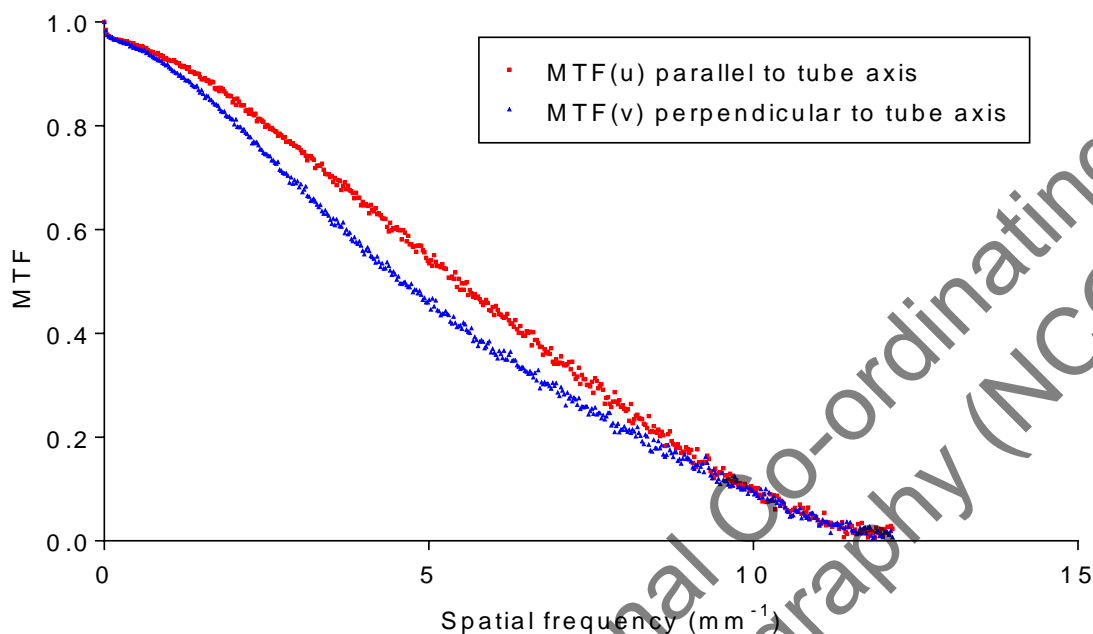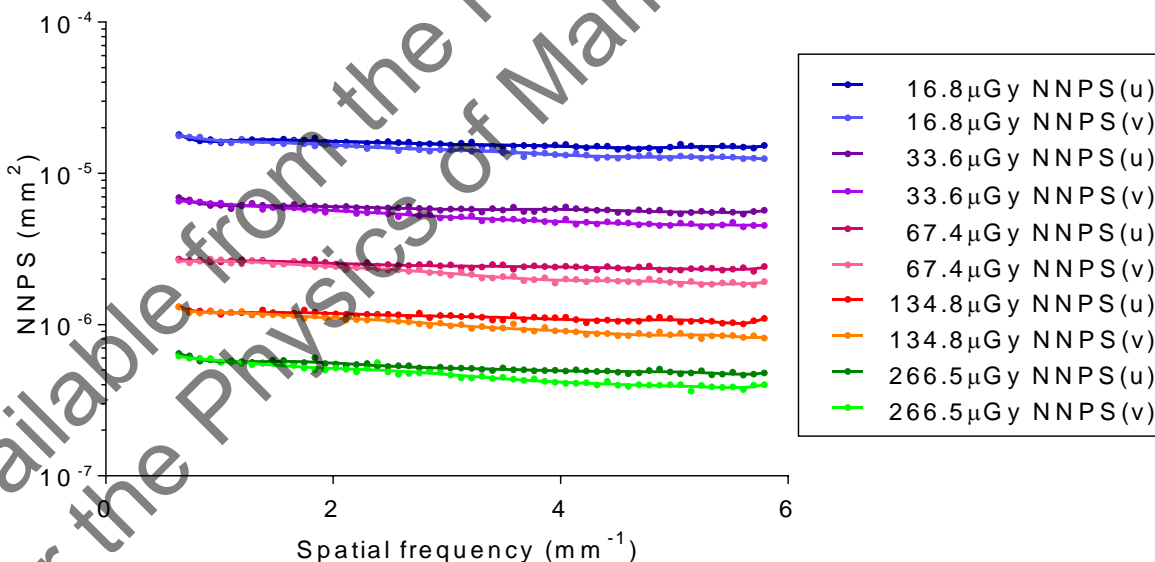

Figure 24. Pre-sampling MTF

Figure 25. NNPS curves for a range of entrance air kerma

Figure 26 shows the DQE averaged in the 2 orthogonal directions for a range of entrance air kerma. The MTF and DQE measurements were interpolated to show values at standard frequencies in Table 14.
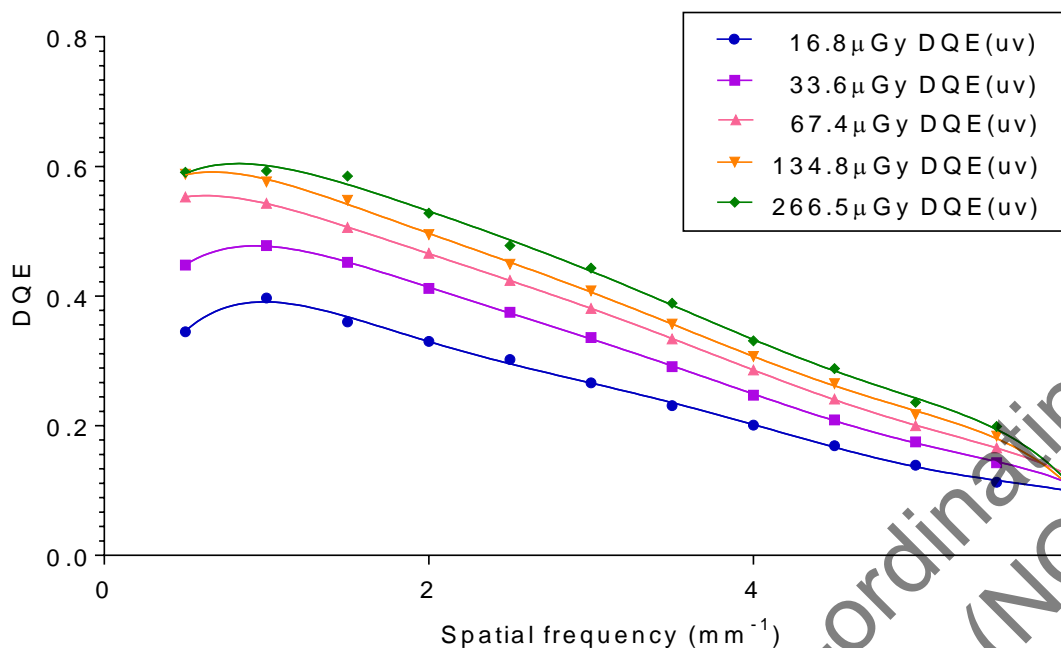
35

Figure 26. DQE averaged in both directions using 29kV W/Rh and a range of air kerma incident at the breast support platform

Table 14. MTF and DQE measurements at standard frequencies (DQE at 67.4µGy)

Frequency (mm^{-1})	MTF (u)	MTF (v)	MTF (uv)	DQE (uv)
0.0	0.97	0.97	0.97	0.358
0.5	0.96	0.95	0.96	0.553
1.0	0.93	0.91	0.92	0.543
1.5	0.89	0.86	0.88	0.506
2.0	0.85	0.81	0.83	0.466
2.5	0.80	0.75	0.78	0.424
3.0	0.76	0.69	0.72	0.381
3.5	0.70	0.62	0.66	0.334
4.0	0.65	0.57	0.61	0.286
4.5	0.60	0.51	0.55	0.241
5.0	0.55	0.46	0.50	0.200
5.5	0.49	0.41	0.45	0.166
6.0	0.45	0.37	0.41	0.116
6.5	0.40	0.33	0.36	0.035
7.0	0.35	0.29	0.32	0.006
7.5	0.30	0.26	0.28	0.001
8.0	0.26	0.22	0.24	0.000
8.5	0.21	0.19	0.20	0.000
9.0	0.17	0.15	0.16	0.000
9.5	0.13	0.12	0.12	0.000
10.0	0.09	0.09	0.09	0.000
10.5	0.06	0.06	0.06	0.000
11.0	0.04	0.04	0.04	0.000
11.5	0.03	0.03	0.03	0.000
12.0	0.03	0.02	0.02	0.000

4. Discussion

Doses measured under AEC control were well within the NHSBSP dose limits for all equivalent breast thicknesses. Five AEC dose levels are available, ranging from 20% below to 20% above the normal dose setting. At the normal dose setting the MGD to a 53mm equivalent breast thickness was 0.89mGy, and at the highest dose setting the MGD was 1.06mGy.

For measurements made using plain PMMA and segmentation off, differences in dose between operating the system in grid mode and using the grid-less PRIME mode ranged from 0% to 15%. When a local dense area (increase in density approximately 20%) was simulated using small pieces of PMMA, with segmentation on, the doses in grid mode increased by between 30% and 70%. When using PRIME, the corresponding increase was between 20% and 40%. At each thickness, with segmentation on, the dose reduction obtained by using PRIME instead of grid mode was approximately 20%. The dose reduction effect of PRIME in clinical use may be different, as the extra thickness used was chosen to demonstrate the effect. PRIME only operates for thicknesses up to 70mm, and the grid is employed for all exposures of larger breasts.

Measurements of image quality using CDMAM showed no significant difference in threshold gold thickness with or without PRIME at a given dose level. At the dose level selected by the AEC for a 60mm equivalent breast thickness, the threshold gold thicknesses were close to the achievable level for all detail diameters.

CNR measurements showed a decrease in CNR with increasing breast thickness. For equivalent breast thicknesses less than 60mm, the CNR exceeded the target level required for the achievable level of image quality. For larger breast thicknesses CNR fell below the achievable level, but remained above the minimum acceptable level.

The high dose setting is recommended for NHSBSP use, in order to bring the CNR for the larger breasts closer to the achievable level of image quality.

The local dense area test showed that a constant SNR was maintained within the dense area by an automatic increase in tube-load, up to a point (10mm PMMA added attenuation to a 30mm PMMA block) beyond which the dense area was excluded by the AEC.

Testing demonstrated how segmentation identifies dense areas in the breast, but excludes dense areas within the pectoral muscle region for mediolateral oblique images acquired at an appropriate angle.

Noise measurements showed that quantum noise dominates the noise for the range of detector doses used clinically. Structural noise appeared to be zero.

5. Conclusions

The Siemens Inspiration system with VB30L software, with or without the PRIME option, meets the main standards in the NHSBSP and European protocols. Doses are well within limits and image quality exceeds the minimum acceptable level when using the AEC at the normal dose level. In order to reach the achievable level of image quality for equivalent breast thicknesses greater than 60mm, which would be preferable, the doses would need to be increased for the larger breasts.

For NHSBSP use we recommend use of the high dose setting. Ideally the AEC curve should be altered so that the achievable level of image quality is met for all equivalent breast thicknesses up to 90mm. Use of PRIME does not affect the image quality at a given dose level, but when PRIME is in use with a phantom containing a local dense area, it has the effect of reducing the dose for equivalent breast thicknesses up to 70mm.

References

1. Kulama E, Burch A, Castellano I et al. *Commissioning and routine testing of full field digital mammography systems* (NHSBSP Equipment Report 0604, Version 3)*. Sheffield: NHS Cancer Screening Programmes, 2009

2. van Engen R, Young KC, Bosmans H et al. European protocol for the quality control of the physical and technical aspects of mammography screening. In *European guidelines for quality assurance in breast cancer screening and diagnosis*, Fourth Edition, Luxembourg: European Commission, 2006

3. van Engen R, Bosmans H, Dance D et al. Digital mammography update: European protocol for the quality control of the physical and technical aspects of mammography screening. In *European guidelines for quality assurance in breast cancer screening and diagnosis,* Fourth Edition – Supplements. Luxembourg: European Commission, 2013

4. Alsager A, Young KC, Oduko JM. Impact of heel effect and ROI size on the determination of contrast-to-noise ratio for digital mammography systems*. In *Proceedings of SPIE Medical Imaging*, Bellingham WA: SPIE Publications, 2008, 691341: 1–11

5. Boone JM, Fewell TR and Jennings RJ. Molybdenum, rhodium and tungsten anode spectral models using interpolating polynomials with application to mammography *Medical Physics,* 1997, 24: 1863–1974

6. Berger MJ, Hubbell JH, Seltzer SM, Chang et al. XCOM: Photon Cross Section Database (version 1.3) http://physics.nist.gov/xcom (Gaithersburg, MD, National Institute of Standards and Technology), 2005

7. Young KC, Cook JH, Oduko JM. Automated and human determination of threshold contrast for digital mammography systems. In *Proceedings of the 8th International Workshop on Digital Mammography,* Berlin: Springer-Verlag, 2006, 4046: 266–272

8. Young KC, Alsager A, Oduko JM et al. Evaluation of software for reading images of the CDMAM test object to assess digital mammography systems. In *Proceedings of SPIE Medical Imaging*, Bellingham WA: SPIE Publications, 2008, 69131C: 1–11

9. IEC 62220-1-2, *Determination of the detective quantum efficiency – Detectors used in mammography.* International Electrotechnical Commission , 2007

10. Dance DR, Young KC, van Engen RE. Further factors for the estimation of mean glandular dose using the United Kingdom, European and IAEA breast dosimetry protocols. *Physics in Medicine and Biology,* 2009*, 54: 4361–4372

11. Young KC, Oduko JM. *Technical evaluation of the Hologic Selenia full field digital mammography system with a tungsten tube* (NHSBSP Equipment Report 0801). Sheffield: NHS Cancer Screening Programmes, 2008

12. Young KC, Oduko JM, Gundogdu O and Asad M. *Technical evaluation of profile automatic exposure control software on GE Essential FFDM systems* (NHSBSP Equipment Report 0903). Sheffield: NHS Cancer Screening Programmes, 2009

13. Young KC, Oduko JM and Asad M. *Technical Evaluation of Agfa DX-M Mammography CR Reader with HM5.0 Needle-IP* (NHSBSP Equipment Report 0905). Sheffield: NHS Cancer Screening Programmes, 2009

14. Young KC, Oduko JM, Gundogdu, O and Alsager, A. *Technical evaluation of Siemens Mammomat Inspiration Full Field Digital Mammography System* (NHSBSP Equipment Report 0909). Sheffield: NHS Cancer Screening Programmes, 2009

15. Young KC, Oduko JM. *Technical evaluation of Hologic Selenia Dimensions 2-D Digital Breast Imaging System with software version 1.4.2* (NHSBSP Equipment Report 1201). Sheffield: NHS Cancer Screening Programmes, 2012

16. Strudley CJ, Young KC, Oduko JM. *Technical Evaluation of the IMS Giotto 3DL Digital Breast Imaging System* (NHSBSP Equipment Report 1301). Sheffield: NHS Cancer Screening Programmes, 2013

17. Oduko JM, Young KC, Warren L. *Technical evaluation of the Fuji Amulet f/s Digital Breast Imaging System* (NHSBSP Equipment Report 1304). Sheffield: NHS Cancer Screening Programmes, 2013

18. Oduko JM, Young KC. *Technical evaluation of Philips MicroDose L30 with AEC software version 8.3* (NHSBSP Equipment Report 1305). Sheffield: NHS Cancer Screening Programmes, 2013

Appendix: Manufacturer's comments

The Siemens Inspiration system can be configured to provide lower or higher dose levels, compared to its default setting, depending on the thickness of the compressed breast and according to the user's diagnostic requirements. This allows adapting to individual preferences regarding dose and image quality. For use in the NHS Breast Screening Programme, it would be possible to configure the system such that higher doses levels would be applied depending on breast thickness, for example to breasts of thickness greater than 60mm.

Image quality measurements for an equivalent breast of 60mm compressed thickness (Section 3.6, Tables 12–13, Figures 20–23) showed similar results for grid mode and scatter correction mode, with the expected dose reduction inside the confidence limits of the measurements. The dose reduction with PRIME depends on the breast thickness, and higher reductions are possible for breasts thinner than 60mm. The results from the adapted test in Section 3.3.4 provide a realistic estimate of the dose saving possible with PRIME in clinical use, especially for thinner breasts. From these measurements an average dose saving of about 20% was determined (Table 9).